ISSN 1070-3284, Russian Journal of Coordination Chemistry, 2015, Vol. 41, No. 6, pp. 395–404. © Pleiades Publishing, Ltd., 2015.

Synthesis, Crystal Structure, Properties, and Nuclease Activity of a New Cu(II) Complex $[Cu(L)_2(Py)_2(H_2O)]$ (HL = *N*-(5-(4-Methylphenyl)-[1,3,4]-Thiadiazole-2-yl)toluenesulfonamide)[1]

A. C. Hangan[a], A. Turza[b], R. L. Stan[a, *], R. Stefan[c], and L. S. Oprean[a]

[a] *Faculty of Pharmacy, University of Medicine and Pharmacy, Cluj-Napoca, 400010 Romania*

[b] *National Institute for R&D of Isotopic and Molecular Technologies, Cluj, 400293 Romania*

[c] *Preclinics Department, University of Agricultural Science and Veterinary Medicine, Cluj-Napoca,400372 Romania*

**e-mail: roxanaluc@yahoo.com*

Received October 24, 2014

Abstract—A new *N*-sulfonamide ligand, *N*-(5-(4-methylphenyl)-[1,3,4]-thiadiazole-2-yl)toluenesulfonamide (HL) and its Cu(II) complex $[Cu(L)_2(Py)_2(H_2O)]$ (**I**), have been synthesized. The X-ray crystal structure of the ligand and of complex **I** have been determined (CIF files CCDC nos. 975153 (HL), 851790 (**I**)). In **I**, the Cu^{2+} ion is five-coordinated, forming a CuN_4O chromophore. The ligand acts as monodentate, coordinating the metal ion through a single $N_{thiadiazole}$ atom. The molecules from the reaction medium (pyridine and water) are also involved in the coordination of the Cu^{2+} ion. Complex **I** has a slightly distorted square pyramidal geometry. The complex was characterized by FT-IR, electronic, EPR spectroscopic and magnetic methods. The nuclease activity studies of the synthesized complex confirm his capacity to cleavage the DNA molecule. The ligand has two important roles in the nuclease activity of I: it influence the reactivity of the Cu^{2+} ion and interact with DNA molecule. The complex interacts with the DNA molecule. Immediately, the Cu^{2+} ion is reduced to Cu(I), and in the presence of molecular oxygen the formed Cu(I) complex produces reactive oxygen species in close proximity to the double helix.

DOI: 10.1134/S1070328415050024

INTRODUCTION

Transition-metal complexes endowed with redox properties and DNA affinity have been developed as chemical cleavers of nucleic acids over the last two decades. Their ability to cleave DNA has several possible applications that include probing structural variations in nucleic acids, identification of binding sites of DNA ligands, design of artificial DNA cleavers and potential chemotherapeutic agents [1–3].

The synthesis of Cu(II) complexes with *N*-substituted heterocyclic sulfonamides greatly increased in the past twenty years due to the diversity of biological activity of the resulting compounds: antimicrobial, anti-inflammatory, the mimetic superoxide dismutase (SOD) or nuclease activity. Studies have shown that Cu(II) complexes with different types of ligands can be used as potential "chemical nucleases" [4–8].

As reported in literature, the ligands commonly used to form complexes with "nuclease activity" are quinolones, sulfonamides and flavonoides. The aromatic rings in the structure of *N*-substituted sulfonamides can be intercalated between the bases of the DNA chain. This interaction, followed by reactive oxygen species (ROS) formation (due to this Cu^{2+} ion in the structure of the complexes) results in degradation of the DNA molecule through an oxidative mechanism [9, 10].

For the past several years, our group has worked on the synthesis of copper-sulfonamide complexes in order to obtain novel antitumor agents. These complexes are especially attractive as anticancer agents because several substituted sulfonamides have been found to arrest the cell cycle, causing apoptosis in the M phase [11]. In this context, we have described the nuclease activity of several copper-sulfonamide complexes [12–15]. In the present paper, we report the synthesis, the crystal structure and the physico-chemical characterization of a new *N*-substituted heterocyclic sulfonamide: HL = *N*-(5-(4-methylphenyl)-[1, 3, 4]-thiadiazole-2-yl)-toluenesulfonamide

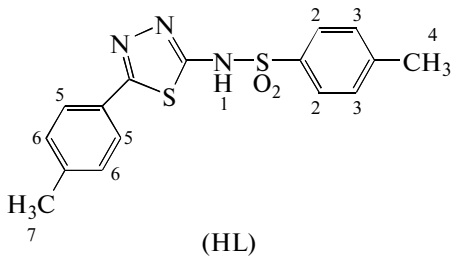

(HL)

[1] The article is published in the original.

One complex of this ligand with Cu(II), $[Cu(L)_2(Py)_2(H_2O)]$ (**I**), was prepared and its structure was determined by X-ray diffraction. Its IR, EPR, electronic spectra and its magnetic susceptibility were investigated and discussed, along with the structural and spectral comparison with those of the analogous complexes. The study of nuclease activity shows his capacity to intercalate in the DNA molecule and the $OH^{\cdot}$ radicals and the $O_2^{-}{}^{\cdot}$ anion radical are the species involved in the cleavage of the DNA molecule.

EXPERIMENTAL

Materials and physical measurements. Copper sulfate pentahydrate, methanol, toluenesulfonylchloride, 2-amino-5-(4-methylphenyl)-[1,3,4]-thiadiazole and pyridine were purchased from Fluka and Merck chemical companies and were used without further purification.

Elemental analyses (C, N, H, and S) were performed with Vario EL analyser. IR spectra were recorded with a Jasco FT/IR-4100 spectrophotometer using diffuse reflectance of incident radiation focused on a sample in the 4000–450 cm^{-1} range. All melting points were determined in open capillaries with an Electrothermal IA 9100 apparatus and were uncorrected. ^1H NMR spectrum of the ligand was recorded at room temperature using DMSO as solvent in 5 mm tubes on Bruker AM 300 NMR spectrometer equipped with a dual, ^1H (multinuclear) head operating at 300 MHz for protons. Fast ion bombardment (FAB) mass spectrum of the ligand was obtained on a VG Autospec spectrometer in *m*-nitrobenzene as a solvent. Diffuse reflectance spectrum of the complex was carried out on a Jasco V-550 spectrophotometer. Magnetic susceptibilitie was measured at room temperature with the Faraday MSB-MKI balance. $Hg[Co(NCS)_4]$ was used as susceptibility standard. Electronic paramagnetic resonance (EPR) spectrum was performed at room temperature with a Bruker ELEXSYS spectrometer operating at the X-band frequency.

Synthesis of HL. A solution containing 1 mmol of 2-amino-5-(4-methylphenyl)-[1,3,4]-thiadiazole and 0.9 mmol of toluenesulfonylchloride in 18 mL of pyridine was heated at reflux for 1 h, at 60°C. The mixture was added to 30 mL of cold water and stirred for several minutes. The resulting solid was recrystallized from ethanol. The yield was 87%; m.p. = 232–234°C.

For $C_{16}H_{15}N_3O_2S_2$ (M = 345)

anal. calcd., %:	C, 55.63;	H, 4.38;	N, 12.16;	S, 18.56.
Found, %:	C, 55.47;	H, 4.26;	N, 12.25;	S, 18.72.

IR (KBr; ν, cm^{-1}): 3260 (N–H), 1544 (C=Car), 1551 (thiadiazole), 1315 ($S=O_{as}$), 1154 ($S=O_s$); 903 (S–N). ^1H NMR (DMSO-d^6; δ, ppm (J, Hz)): 2.37–2.36 (6H, s., H-4, H-7), 7.38–7.34 4H, d., J = 7.8, H-5, H-2), 7.73–7.71 (4H, d., J = 7.8, H-6, H-3), 8.52 (1H, s., H-1). MS (*m/z*): 346 [M + H^+].

Synthesis of complex I. A solution of $CuSO_4 \cdot 5H_2O$ (4 mmol) in 20 mL of pyridine–H_2O (V : V = 1 : 1) was added dropwise under continuous stirring to a solution of HL ligand (1 mmol) dissolved in 25 mL pyridine–H_2O (V : V = 2 : 3). The resulting solution was stirred at room temperature for 2 h and left to stand at room temperature. After two months by the slow evaporation of the solvent, green-blue crystals suitable for X-ray diffraction were obtained. The yield was ~58%.

For $C_{42}H_{40}N_8O_5S_4Cu$ (M = 928.61)

anal. calcd., %:	C, 54.31;	H, 4.31;	N, 12.06;	S, 13.79.
Found, %:	C, 54.20;	H, 4.22;	N, 12.21;	S, 13.85.

IR (KBr; ν, cm^{-1}): 1488 (thiadiazole); 1296 ($S=O_{as}$), 1125 ($S=O_s$), 927 (S–N). UV-Vis (solid; λ_{max}, nm): 314 ($\pi \rightarrow \pi^*$), 401(LMCT), 583 (d–d).

X-ray crystallography. A white crystal of the ligand (HL), size 0.25 × 0.21 × 0.15 mm was mounted on a glass fiber and used for data collection. Crystal data were collected at 293(2) K using a dual microsourse Supervova Diffractometer and MoK_α radiation (λ = 0.71073 Å). A blue crystal of **I** was mounted on a glass fiber and used for data collection. Crystal data were collected at 293(2) K using a dual microsourse Supervova Diffractometer and CuK_α radiation (λ = 1.54184 Å).

The data were processed with CrysAlisPro [16] and corrected for absorbtion using ABSPACK [17]. The structure was solved by direct methods using the program SHELXS-97 [18] and refined by full-matrix least-squares techniques against F^2 using SHELXL-97 [19]. Both SHELXS-97 and SHELXL-97 are incorporated in Olex2 [20] software package. Positional and anisotropic atomic displacement parameters were refined for all nonhydrogen atoms. Hydrogen atoms were located in difference maps and included as fixed contributions riding on attached atoms with isotropic thermal parameters. Atomic scattering factors were from International Tables for Crystallography [21]. Molecular graphics were from PLATON [22] and SCHAKAL [23]. A summary of the crystal data, experimental details and refinement results is listed in Table 1.

Supplementary material has been deposited with the Cambridge Crystallographic Data Centre (nos. 975153 (HL), 851790 (**I**); deposit@ccdc.cam.ac.uk or http://www.ccdc.cam.ac.uk).

DNA cleavage. Reactions were performed by mixing 7 μL of cacodylate buffer 0.1 M, pH 6 (cacodylic acid/sodium cacodylate), 6 μL of complex solution (final concentrations: 3, 6, 9, 12 and 15 μM), 1 μL of pUC18 DNA solution (0.25 μg/μL, 750 μM in base pairs), and 6 μL of activating agent solution (H_2O_2–ascorbic acid) in a threefold molar excess relative to

Table 1. Crystal data, experimental details and refinement results for HL and complex **I**

Parameter	Value	
Formula weight	345.44	928.61
Temperature, K	293(2)	293(2)
Crystal system	Triclinic	Monoclinic
Space group	$P\bar{1}$	$P/n2$
a, Å	6.5667(4)	15.0977(3)
b, Å	10.6561(10)	21.7903(4)
c, Å	13.5350(16)	13.1399(2)
α, deg	67.598(10)	90
β, deg	88.551(8)	103.3750(17)
γ, deg	72.139(7)	90
Volume, Å^3	828.91(13)	4205.56(8)
Z	2	4
ρ_{calcd}, mg/m^3	1.432	1.468
Absorption coefficient, mm^{-1}	0.336	3.049
F(000)	372	1928
Crystal size, mm	0.25 × 0.21 × 0.15	0.37 × 0.14 × 0.07
θ Range for data collection, deg	6.28–58.14	3.46–74.78
Limiting indices	$-8 \le h \le 8$, $-14 \le k \le 14$, $-17 \le l \le 18$	$-14 \le h \le 18$, $-26 \le k \le 22$, $-16 \le l \le 11$
Collected reflections	6166	8243
Independent reflections (R_{int})	3755 (0.0444)	3998 (0.0575)
Completeness to θ = 27.48, %	99.90	99.92
Data/restraints/parameters	3755/0/210	5127/6/552
Goodness-of-fit on F^2	1.152	1.019
Final R indices ($I > 2\sigma(I)$)	$R_1 = 0.0732$, $wR_2 = 0.1934$	$R_1 = 0.0523$, $wR_2 = 0.1314$
R indices (all data)	$R_1 = 0.1119$, $wR_2 = 0.2329$	$R_1 = 0.1125$, $wR_2 = 0.1748$
$\Delta\rho_{max}/\Delta\rho_{min}$, e Å^{-3}	0.44/–0.42	0.183/–0.191

the concentration of the complex. The resulting solutions were incubated for 1 h at 37°C, after which a quench buffer solution (3 μL) consisting of bromophenol blue (0.25%), xylene cyanole (0.25%) and glycerol (30%) was added. The solution was then subjected to electrophoresis on 0.8% agarose gel in 0.5× TBE buffer (0.045 M Tris, 0.045 M boric acid, and 1 mM EDTA) containing 5 μL/100 mL of a solution of ethidium bromide (10 mg/mL) at 100 V for 2 h. The bands were photographed on a capturing system (Gelprinter Plus TDI).

To test for the presence of ROS generated during strand scission and for possible complex-DNA interaction sites, various reactive oxygen intermediate scavengers and groove binders were added to the reaction mixtures. The scavengers used were 2,2,6,6-tetramethyl-4-piperidone

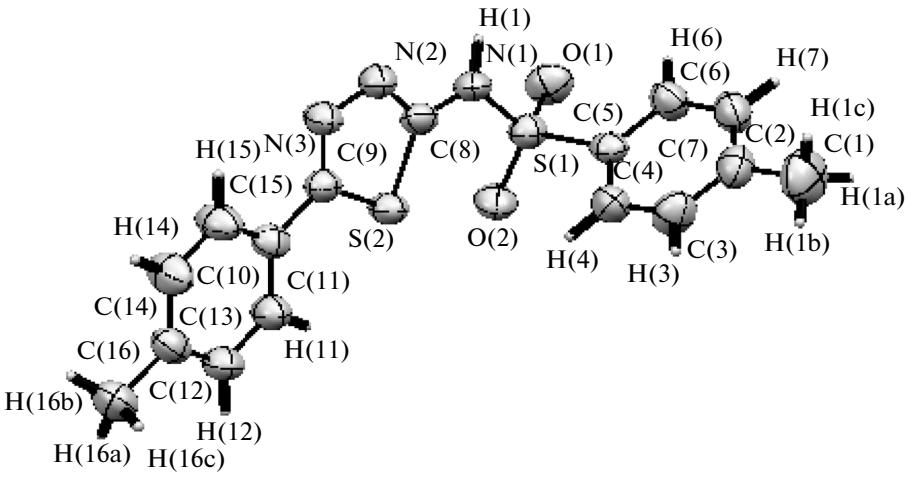

Fig. 1. ORTEP drawing of ligand HL.

(0.5 M), DMSO (14 M), *t*-butyl alcohol (10.5 M), NaN_3 (400 mM), superoxide dismutase (SOD; 15 units). In addition, a chelating agent of copper(I), neocuproine (36 μM), along with the groove binder distamycin (80 μM) were also assayed. Samples were treated as described above.

RESULTS AND DISCUSSION

Relevant bond distances and angles for the molecule HL are collected in Table 2. The molecular structure and crystallographic numbering scheme are illustrated in Fig. 1. Interpretation of the crystallographic data is carried out by comparison with data available from methazolamide ligands and 5-amino-1,3,4-thiadiazole-2-sulfonamide [24, 25].

The resulting structure for the thiadiazole ring is planar. The bond distance between the C(9)–N(3) atoms is 1.296 Å, typical for a double bond. The C(8)–N(2) bond length is larger (1.345 Å), due to the delocalization of charge on these atoms and the adjacent N(1) atom in the sulphonamidic group. Nevertheless, the C(8)–N(2) and C(8)–N(1) bonds, the latter of 1.319 Å, are shorter than a C–N single bond (1.416 Å for N(sp^3). Also, due to the delocalization of charge in the thiadiazole ring and sulfanilamido group, the N(2)–N(3) bond of 1.369 Å is lower than N–N single bond (1.420 Å).

On the other hand, the C–S bonds of the thiadiazole ring, C(9)–S(2) (1.746 Å) and C(8)–S(2) (1.729 Å), are essentially equal and similar to the thiophene ring [26]. This indicated a marked character π of the bonds, resulting as a delocalization of the negative charge density through the thiadiazole ring.

The sulfur atom (S(1)) of the sulfonamide group shows a distorted tetrahedral geometry, the largest deviation occurs at the O(1)S(1)O(2) angle of 118.7°, while the other angles have values between 104°–111°. The distances between the sulfur and oxygen atoms in S(1)–O(1) and S(1)–O(2) bonds are 1.424 and 1.441 Å, typical for double bonds. The N(1)–S(1) length of 1.612 Å, is consonant with data obtained for other sulfonamides with similar structure [27]. The geometry of the N(1) atom of the sulfonamide group is trigonal planar, as shown by the values of the angles between neighboring atoms: H(1)N(1)S(1) (120°), H(1)N(1)C(8) (119°) and C(8)N(1)S(1) (121°).

The S(1)–C(5) bond (1.766 Å) is the largest of all bonds in the molecule and indicates the of π interactions between the sulfonamide group and the toluene's ring.

The C–C bond lengths of the two toluene rings in the sulfonamidic molecule are between 1.362 and 1.394 Å and are intermediate between a single and a double bond. The distances C(13)–C(16) and C(1)–C(2), 1.517 and 1.518 Å, respectively, indicate the existence of σ bond between these atoms.

Relevant bond distances and angles for complex **I** are collected in Table 2. The molecular structure and crystallographic numbering scheme are illustrated in Fig. 2.

Complex **I** contains a CuN_4O entity in a slightly distorted square pyramidal geometry. In the basal (equatorial) plane Cu^{2+} ion is coordinated by two nitrogen atoms of the two thiadiazole rings (N(2a) and N(2b)) from the sulfonamidate ligands and two nitrogen atoms from each pyridine molecules (N(1) and N(2)). The Cu(1)–$N_{thiadiazole}$ lengths (Cu(1)–N(2a) 2.004(3) and Cu(1)–N(2b) 2.026(3) Å) are similar to those corresponding to the other complexes with sulphonamide ligands containing a thiadiazole ring [8, 28, 29]. Cu(1)–$N_{pyridine}$ lengths (Cu(1)–N(1) 2.025(4) and Cu(1)–N(2) 2.023(3) Å) are consonant with those measured for similar compounds [8]. One water O atom occupies the axial position with a bond length of 2.316(3) Å. The angles between the atoms in the ecuatorial plane are of about 90° (88.2(1)°–91.2(1)°) and those between the atoms on the axial plane and

Table 2. Selected bond lengths (Å) and angles (deg) for HL and complex **I**

Bond	*d*, Å	Bond	*d*, Å
		HL	
N(1)–S(1)	1.612(5)	C(8)–N(2)	1.345(6)
N(1)–C(8)	1.319(5)	C(9)–N(3)	1.296(7)
S(1)–O(1)	1.424(3)	N(3)–N(2)	1.369(5)
S(1)–O(2)	1.441(4)	C(9)–S(2)	1.746(4)
S(1)–C(5)	1.766(3)	C(8)–S(2)	1.729(5)
		I	
Cu(1)–N(1)	2.025(3)	Cu(1)–N(2b)	2.026(3)
Cu(1)–N(2)	2.023(3)	Cu(1)–O	2.316(3)
Cu(1)–N(2a)	2.004(3)		
Angle	ω, deg	Angle	ω, deg
		HL	
N(1)S(1)O(1)	107.1(2)	N(1)C(8)S(2)	130.6(3)
N(1)S(1)O(2)	111.1(2)	S(1)N(1)C(8)	121.1(3)
N(1)S(1)C(5)	104.1(2)	C(5)S(1)O(2)	107.5(2)
O(1)S(1)O(2)	118.7(2)	C(5)S(1)O(1)	107.3(2)
N(1)C(8)N(2)	120.5(4)		
		I	
N(1)Cu(1)N(2)	166.4(1)	N(2a)Cu(1)N(2b)	176.3(1)
N(1)Cu(1)N(2a)	91.1(1)	N(1)Cu(1)O	96.3(1)
N(1)Cu(1)N(2b)	88.6(1)	N(2)Cu(1)O	97.3(1)
N(2)Cu(1)N(2a)	88.2(1)	N(2a)Cu(1)O	90.5(1)
N(2)Cu(1)N(2b)	91.2(1)	N(2b)Cu(1)O	93.2(1)

the ecuatorial plane are similar (90.5(1)°–97.3(1)°). The distances almost equal between Cu(1) and N atoms in the ecuatorial plane, the distance significantly bigger between Cu(1) and O atom in the axial plane and the angles forming the coordination polyhedron confirm the slightly distorted square pyramidal structure for the complex $[Cu(L)_2(Py)_2(H_2O)]$. The bond length change is described by the tetragonality (T^5). The tetragonality values, 0.87 for the compound, fit into the range expected for square pyramidal complex [26]. The in-plane angular distorsions described by the ratio τ represent a percentage of trigonal distortion of

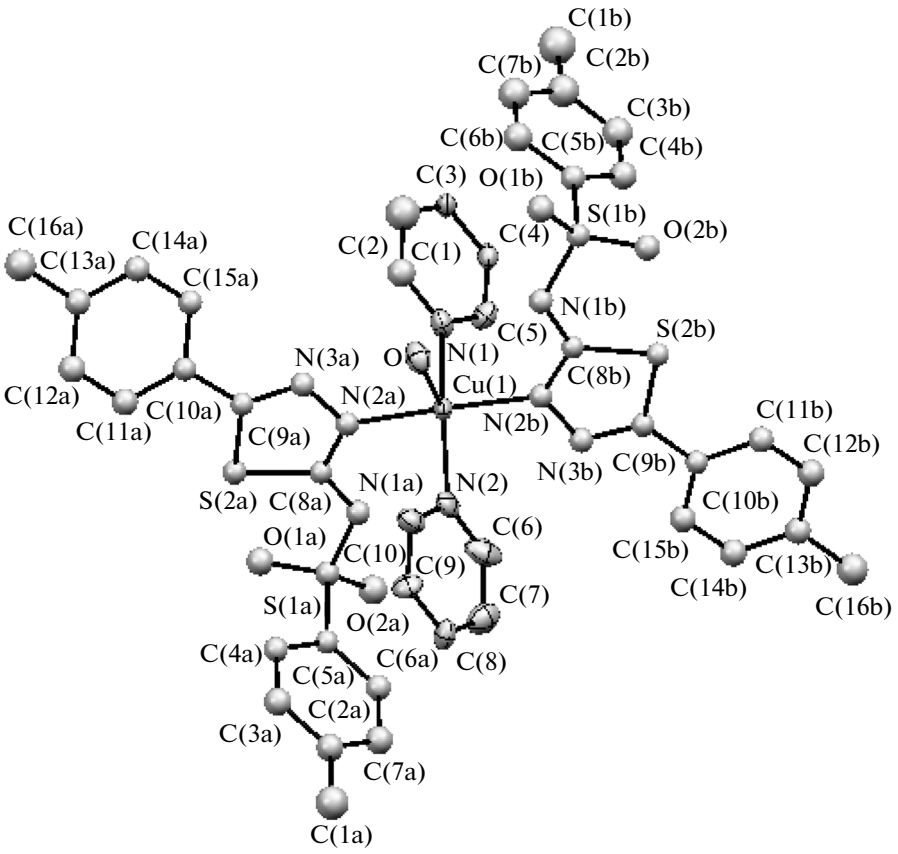

Fig. 2. ORTEP drawing of the $[Cu(L)_2(Py)_2(H_2O)]$ complex.

a square-pyramidal geometry [30]. The τ value of 0.165 for **I** indicates a very slight distortion. It is noteworthy that the coordination of Cu^{2+} ion takes place through the $N_{thiadiazole}$ (N(2a) and N(2b)) atom instead through the deprotonated $N_{sulfonamido}$ (N(1a) and N(1b)) atom. This is a consequence of the charge dellocalization between the sulfonamido and the thiadiazole ring. The sulfonamidate ligand (L^-) acts as monodentate as it coordinates through a nitrogen atom of the thiadiazole heterocycle. The sulfonamide molecules of this type can behave as bidentate ligands as well through the N atom from the thiadiazole moiety and through one of the O atoms and even through the $N_{sulfonamido}$ atom from the sulfonamido moiety [27]. As it is expected the pyridine and the water molecules participate in the coordination as monodentate ligands.

The experimentally observed Fourier transform infrared (FT-IR) peaks of the complex are compared with the obtained spectra for the starting materials: pyridine and HL. Infrared bands, related to ligand and pyridine molecules, are present in the obtained crystal spectrum and prove the raw materials presence in the final structure as described through XRD analysis.

Literature indicates that the bands corresponding to the uncoordinated pyridine molecules appear at 3083, 3055, 3030 (q(C–H)); 1581, 1573, 1481, 1437 (q(C–C), β(CCH)); 1292, 1226 (β(NCH)); 1216, 1145, 1081, 1067 (β(CCH)); 991 (q(N–C)); 973, 940, 883, 748 (χ(N–C)); 704 (ρ(C–H)); 653 (γ(NCC)); 604 cm^{-1} (γ(NCC)) [31].

In spectrum of **I**, the bands related to pyridine only exist; they appear at the same wavenumber ~994 and ~1070 cm^{-1}, but at the same time there are bands with different spectral position than in intial compound spectrum situated at 1043, 1446 1488 cm^{-1}. The shift of the bands assigned to ν(C–C) in pyridine from 1034, 1039, 1483 cm^{-1} to the above mentioned position ilustrated that external environment influence upon that ring.

The most remarkable difference between the IR spectrum of the ligand and the IR spectrum of **I** occurs in the band corresponding to the stretching vibration of the thiadiazole ring, which is shifted from 1550 cm^{-1} (HL) in the free ligand to 1488 cm^{-1} in **I**. The characteristic band corresponding to the ν(S–N) (927 cm^{-1}) in the complex shifted to higher frequencies with respect to those of the uncoordinated HL (920 cm^{-1}). The characteristic band corresponding to the ν(N–N) (1181 cm^{-1}) in the complex shifted to higher frequencies with respect to those of the uncoordinated ligand

HL (1152 cm^{-1}). These modifications in the thiadiazole heterocycle and in the sulfonamide group are attributed to the involvement to the $N_{thiadiazole}$ atom in coodination of Cu(II) and to the deprotonation of the sulfonamido moiety for the complex [32]. Bands due to the antisymmetric and symmetric vibration modes of the S=O bond appear at 1296 and 1128 cm^{-1} in the IR spectrum of **I**, that is lower (~15 cm^{-1}) than those corresponding to the free ligand; such a decrease can be related to the electron transfer from the deprotonated, negatively charged N atom to the sulfonyl oxygen atoms, which results in partial single-bond character for the S–O bonds [33–35]. The lack of bands close to 3200 cm^{-1}, which were originally present in the spectra of the free ligands confirms the deprotonation of the N–H bonds. This deprotonation of the $N_{sulfonamido}$ atom causes a weak conjugation effect among the three N, S, O atoms of the moiety.

In final complex spectrum, there are bands related to the ligand only which changed their spectral position because of the new environment where the atoms are bonded. For instance, bands at 1274, 1296, 1306 cm^{-1} in **I** are shifted to lower wave number when compared with the ligand and their relative intensity has been changed after crystallization.

The other bands can be attributed to pyridine, as they sometimes overlap the frequencies corresponding to moieties of the ligand. The features of the IR spectrum of the complex are similar to those reported for the other copper N-sulfonamide derivatives [10, 34, 36] and demonstrate the existence of new linkages within the complex.

The solid electronic spectrum of **I** displays a band at 401 nm assigned to a LMCT transition. The complex exhibits a *d–d* band at 583 nm. This pattern, characteristic for a distorted square-pyramidal geometry, agrees well with the crystallographic data [37].

The polycrystalline X-band EPR spectrum of the complex is axial. The EPR parameters, obtained by simulation are $g_{\|} = 2.31$, $g_{\perp} = 2.076$ and $A_{\|} = 159 \times 10^{-4}$ cm^{-1} for complex (Fig. 3) [38]. According to the Bertini classification, the value of $A_{\|}$ can be correlated with the geometry of the complex [39]. Thus, A values between 160 and 200 $\times 10^{-4}$ cm^{-1} correspond to a square-planar geometry and the values between 130 and 160 cm^{-1} correspond to a square pyramidal or distorted trigonal bipyramidal geometry. As $g_{\|} > g_{\perp}$ in the complexes, the unpaired electron must be in the $d_{x^2-y^2}$ (or d_{xy}) orbital [40].

The room temperature mesurements of the magnetic moments of complex **I** ($\mu_{eff} = 1.83$ μ_B) are consistent with the presence of a single unpaired electron.

It is known that the DNA cleavage is controlled by relaxation of the supercoiled circular conformation of pUC18 DNA to the nicked circular and/or linear conformations. When electrophoresis is applied to plasmid DNA, the fastest migration will be observed for DNA of the closed circular conformation (**Form I**), if one strand is cleaved, the supercoiled conformation will relax to produce a slower-moving nicked conformation (**Form II**). If both strands are cleaved, a linear conformation (**Form III**) will be generated that migrates in between.

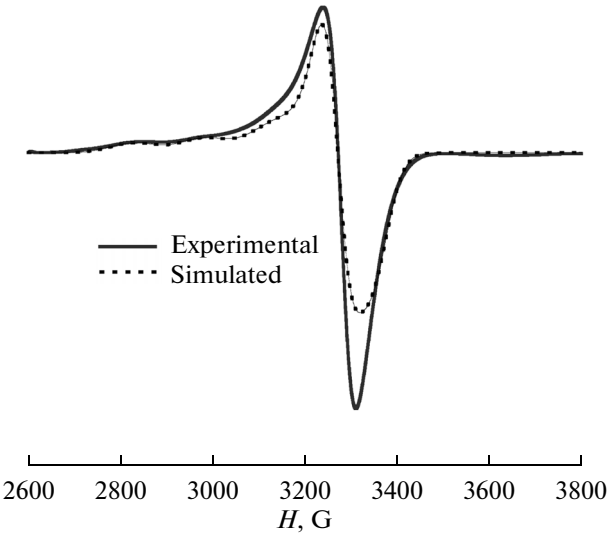

Fig. 3. FT-IR spectrum of complex **I**.

The ability of the complexes to cleave DNA was assayed with the aid of gel electrophoresis on supercoiled pUC18 DNA in DMF: cacodylate buffer (0.1 M, pH 6.0) a molar proportion (1 : 39) in the presence of H_2O_2/ascorbic acid, 3.0-fold excess relative to the complex concentration. Control experiments with $CuSO_4$ were also carried out under the same experimental conditions. The obtained results are presented in Fig. 4. In the presence of the control (pUC18 plasmid in cacodilate buffer) or of the control with reducing agents, there is no nuclease activity (lanes 2 and 3).

It appears that complex **I** can destroy the DNA molecule in stages, forming the circular form at a concentration of 18 μM and then the linear form of the DNA molecule at the concentration of 24 and 30 μM. In the case of the last two concentrations, the circular and linear form coexist (lane 12 and 13), while at 18 μM the circular and the helicoidal form coexist (lane 11). Initially, the cleavage is realized in a single point of a DNA chain, leading to the circular form. Later, a second cleavage occurs in another point of the chain, leading to the linear form.

The copper salt, $CuSO_4 \cdot 5H_2O$, 18 μM, starts to destroy the DNA chain, leading to the circular form, which also appears at higher concentrations (24 and 30 μM). Comparing the nuclease activity of $CuSO_4 \cdot 5H_2O$ (lanes 7 and 8) at the same concentrations with those of the complex (lanes 12 and 13), it can be observed that the latter has a superior nuclease activity. According to the

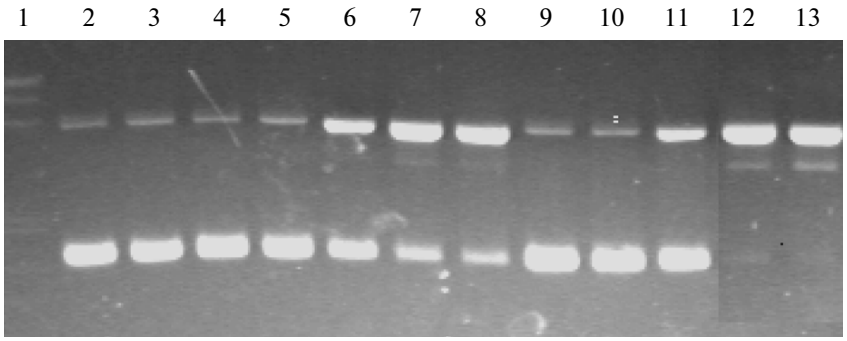

Fig. 4. Electrophoregram in agarose gel of the pUC18 plasmid treated with the $[Cu(L)_2(Py)_2(H_2O)]$ complex: base marker (1); control (2); control with reducing agents (3); $CuSO_4 \cdot 5H_2O$ 6 μM (4), 12 (5), 18 (6), 24 (7), 30 μM (8); complex 6 μM (9), 12 (10), 18 (11), 24 (12), 30 μM (13).

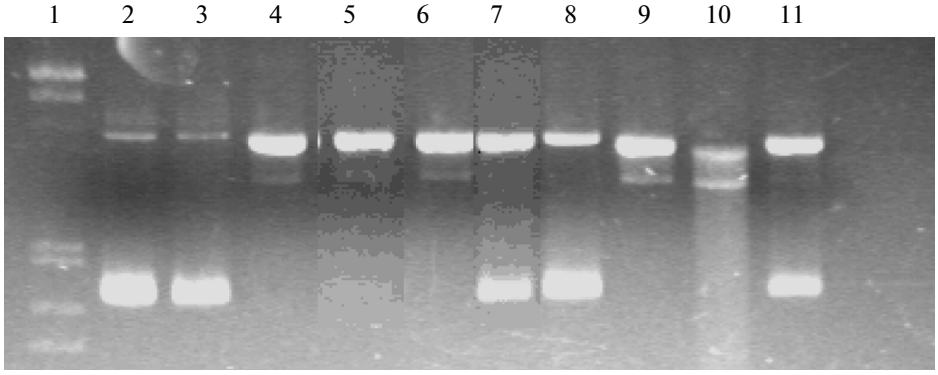

Fig. 5. Electrophoregram in agarose gel of the pUC18 plasmid treated with the $[Cu(L)_2(Py)_2(H_2O)]$ complex and various inhibiting agents: base marker (1); control (2); control with reducing agents (3); complex 30 μM without inhibitors (4); complex 30 μM with: NaN_3 (5); piperidone (6); DMSO (7); *t*-butyl alcohol (8); distamycin (9); SOD (10); neocuproine (11).

analysis of the same electrophoresis, it can be deduced that the nuclease activity of the complex depends on its concentrations. Thus, its capacity to degrade DNA rises with the increase of complex concentration.

The coordination of the Cu^{2+} ion with the sulfonamide deprotonated ligand HL facilitates the destruction of the DNA molecule. Due to the plane aromatic rings from its structure, the sulfonamide allows that the complex molecule be intercalated between base pairs in the DNA chains. This phenomenon is followed by the destruction of the nucleic acid, caused by the production of reactive species of oxygen in its close vicinity [33, 41]. The direct influence of the nuclearity of the copper(II) complexes on their nuclease activity has previously been showed in [41, 42].

The involvement of ROS, such as hydroxyl, superoxide, singlet oxygen-like species and hydrogen peroxide in the nuclease mechanism, was determined by monitoring the quenching of the DNA cleavage in the presence of ROS scavengers. To clarify other aspects of the mechanism, the copper(I)–chelator (neocuproine) and the minor groove binder distamycin were also used. The assays were performed with H_2O_2/ascorbic acid (in a 3.0-fold molar excess relative to complex concentration) as an activating agent. The results for **I** are shown in Fig. 5.

The influence of the inhibitors on the nuclease activity of the complex can be observed in the fact that sodium azide and 2,2,6,6-tetramethyl-4-piperidone (lanes 5 and 6) do not greatly modify the nuclease activity of the complex. This proves the fact that the singlet oxygen $^1O_2$ does not participate in the destruction of the DNA.

In the presence of DMSO and of *t*-butyl alcohol (lanes 7 and 8), we can observe a decrease in the degradation of the DNA molecule. This can be explained by the presence of the OH· radicals in the destruction process of the nucleic acid, as the two inhibitors act by capturing these radicals, thus decreasing their concentration and consequently the nuclease activity of the complex.

By adding distamycin (lane 9), the nuclease activity of **I** is slightly increased. This proves that its activity is not similar with that of distamycin – a binder of the minor groove of DNA.

The SOD enzyme leads to a significant increase of the nuclease activity of the complex (line 10). This can

be noticed from an increase of the amount of linear DNA in this sample as compared to the complex sample without SOD (lane 4). This enzyme catalyzes the dismutation of the superoxide anion radical $O_2^{\bullet-}$, leading to H_2O_2 and O_2, which can further produce active species which participate in the destruction of DNA.

In the presence of neocuproine (lane 11), the capacity of the complex to destroy DNA is much reduced (the helicoidal and circular form coexist). In the case of the studied complex, this can be explained by the reduction of the Cu^{2+} ion to Cu(I) as intermediate step in the DNA degradation process. By adding neocuproine, a stable complex of Cu(I) is formed (Cu(I)-neocuproine), thus inhibiting the subsequent reactions of the degradation mechanism of the DNA molecule.

Hydroxyl radicals are generated by a variety of chemical and physical processes. Transition-metal mediated $^{\bullet}OH$ production is known to occur by a number of routes; two well known pathways are the Fenton [43] and the Haber–Weiss [44] mechanisms. The complex interacts with the DNA molecule. Immediately, the Cu^{2+} ion is reduced to Cu(I), and in the presence of the molecular oxygen, the formed Cu(I) complex produces reactive oxygen species in close proximity to the double helix. These species finally attack the 2-deoxyribose moiety, leading to the cleavage of the DNA chain. If the reactive species are not formed close to DNA, they are likely to be dispersed and neutralized.

ACKNOWLEDGMENTS

Adriana Hangan is thankful for the financial support offered by research grant Resurse Umane PNII-PD 474/2010.

REFERENCES

1. Liu, C., Zhou, J., Li, Q., et al., *J. Inorg. Chem.*, 1999, vol. 75, p. 233.
2. Theodorou, A., Demertzis, M.A., and Kovala-Demertzis, D., *Biometals*, 1999, vol. 12, p. 167.
3. Sigman, D.S., Kuwabara, M.D., Chen, C.H., et al., *Methods Enzymol.*, 1991, vol. 208, p. 414.
4. Gonzalez-Alvarez, M., Alzuet, G., Borras, J., et al., *Inorg. Chem.*, 2003, vol. 42, p. 2992.
5. Gonzalez-Alvarez, M., Alzuet, G., Borras, J., et al., *J. Biol. Inorg. Chem.*, 2003, vol. 8, p. 644.
6. Marcias, B., Garcia, I., Villa, M.V., et al., *Inorg. Chim. Acta,* 2003, vol. 353, p. 139.
7. Garcia-Gimenez, J.L., Alzuet, G., Gonzalez-Alvarez, M., et al., *J. Inorg. Chem.*, 2007, vol. 46, p. 7178.
8. Hangan, A., Borras, J., Liu-Gonzalez, M., et al., *Z. Anorg. Allg. Chem.*, 2007, vol. 633, p. 1837.
9. Gonzalez-Alvarez, M., Alzuet, G., Borras, J., et al., *J. Biol. Inorg. Chem.*, 2008, vol. 13, p. 1249.
10. Thomas, A.M., Nethaji, M., Chakravarty, A.R., *J. Inorg. Biochem.*, 2004, vol. 98, p. 1087.
11. Owa, T., Yoshino, H., Okauchi, T., et al., *J. Med. Chem.*, 1999, vol. 42, p. 3789.
12. Cedujo, R., Alzuet, G., Gonzalez-Alvarez, M., et al., *J. Inorg. Biochem.*, 2006, vol. 100, p. 70.
13. Gonzalez-Alvarez, M., Alzuet, G., Castillo-Agudo, L., et al., *Eur. J. Inorg. Chem.*, 2006, vol. 19, p. 3823.
14. Marcias, B., Villa, M.J., Gomez, B., et al., *J. Inorg. Biochem.*, 2006, vol. 101, p. 444.
15. Garcia-Gimenez, J.L., Alzuet, G., Gonzalez-Alvarez, M., et al., *J. Inorg. Biochem.*, 2009, vol. 103, p. 243.
16. *CrysAlis PRO CCD and CrysAlis PRO RED*, Oxford Diffraction Ltd., Abingdon, 2006.
17. *SCALE3 ABSPACK, Empirical Absorption Correction, CrysAlis–Software Package*, Oxford Diffraction Ltd., 2006.
18. Sheldrick G.M., *SHELXS-97, Program for Crystal Structure Solution*, Göttingen (Germany): Univ. of Göttingen, 1997.
19. Sheldrick G.M., *SHELXL-97, Program for the Refinement of Crystal Structures*, Göttingen (Germany): Univ. of Göttingen, 1997.
20. Dolomanov, O.V., Bourhis, L.J., Gildea, et al., *J. Appl. Cryst.*, 2009, vol. 42, p. 339.
21. Wilson A.J.C., *International Tables for Crystallography*, vol. C, Dordrecht (The Netherlands): Kluwer Academic Publishers, 1995.
22. Spek A.L., *PLATON, A Multipurpose Crystallographic Tool*, Utrecht (The Netherlands): Utrecht Univ., 2000.
23. Keller E., *SCHAKAL-97, A Computer Program for the Graphic Representation of Molecular Crystallographic Models*, Freiburg (Germany): Univ. of Freiburg, 1997.
24. Alzuet, G., Ferrer, S., and Borras, J., *Acta Crystallogr., C*, 1991, vol. 47, p. 2377.
25. Pedregosa, J.C., Alzuet, G., and Borras, J., *Acta Crystallogr., C*, 1993, vol. 49, p. 630.
26. Allen, A.M., Kennard, O., Watson, D.G., et. al. *Trans. Perkin* 2, 1987, p. S1.
27. Borras, E., Alzuet, G., Borras, J., et al., *Polyhedron*, 2000, vol. 19, p. 1859.
28. Ferrer, S., Haasnoot, J.G., Graaf, R.A.G., et al., *Inorg. Chim. Acta,* 1992, vol. 192, p. 129.
29. Graf, M., Greaves, B., and Stoeckli-Evans, H., *Inorg. Chim. Acta*, 1993, vol. 204, p. 239.
30. Adison, A.W., Rao, T.N., Reedijk, J., et al., *Dalton Trans.*, 1984, p. 1349.
31. Koon, N., Wong, S., and Colson, D., *J. Mol. Spectrosc.*, 1984, vol. 104, p. 129.
32. Gonzalez-Alvarez, M., Alzuet, G., Borras, J., et al., *J. Inorg. Biochem.*, 2004, vol. 98, p. 189.
33. Marcias, B., Garcia, I., Villa, M.V., et al., *J. Inorg. Biochem.*, 2003, vol. 96, p. 367.
34. Cami, G.E., Ramirez de Arellano, M.C., Fustero, S., et al., *An. Asoc. Quim. Argent.*, 2006, p. 941.
35. Otter, C.A., Couchman, S.M., Jeffery, J.C., et al., *Inorg. Chim. Acta*, 1998, vol. 278, p. 178.
36. Alzuet, G., Ferrer, S., Borras, J., et al., *Inorg. Chim. Acta,* 1993, vol. 203, p. 257.

37. Hathaway, B.J., In: *Comprehensive Coordination Chemistry,* ch. 9, Wilkinson, G., Gillard, R.D., McCleverty, J.A., Eds., New York: Pergamon, 1987.
38. *WINEPR-Simfonia 1.25*, Karlsruhe: Bruker Analytik GmbH, 1994–1996.
39. Bertini, I. and Drago, R., *ESR and NMR of Paramagnetic Species in Biological and Related Systems,* Dordrecht: D. Reidel, 1979.
40. Gonzalez-Alvarez, M., Alzuet, G., Borras, J., et al., *J. Inorg. Biochem.*, 2002, vol. 89, p. 29.
41. Li, L., Karlin, K.D., and Rokita, S.E., *J. Am. Chem. Soc.*, 2005, vol. 127, p. 520.
42. Humphreys, K.J., Karlin, K.D., and Rokita, S.E., *J. Am. Chem. Soc.*, 2002, vol. 124, p. 8055.
43. Pamatong, F.V., Detmer, C.A. III, and Bocarsly, J.R., *J. Am. Chem. Soc.*, 1996, vol. 118, p. 5339.
44. Detmer, C.A. III, Pamatong, F.V., and Bocarsly, J.R., *Inorg. Chem.*, 1996, vol. 35, p. 6292.